

# Effect of Air Damping on the Dynamics of Nonuniform Deformations of Microstructures

Yao-Joe Yang, Marc-Alexis Gretillat\* and Stephen D. Senturia

Department of Electrical Engineering and Computer Science,  
Massachusetts Institute of Technology, Cambridge MA, USA, yjy@mtl.mit.edu

\*Institute of Microtechnology, University of Neuchâtel, Neuchâtel, Switzerland

## ABSTRACT

In this paper, we present a methodology for extracting macromodel parameters of compressible isothermal squeezed-film damping (CISQFD) for *flexible* structures of MEMS under small amplitude oscillation. The theoretical derivation, which is based on structural modal analysis and CISQFD numerical simulation, is presented. The spring and damping components of CISQFD of any oscillation mode can be extracted by this methodology, and thus the generic parameters of CISQFD can be obtained for any flexible structure with given oscillation modes. We successfully formulated an accurate and concise second order dynamics equation for a flexible MEMS devices by using the CISQFD parameters and the modal spring constant and mass. Simulation results of resonance shift and quality factor are consistent with experimental results.

**Keywords:** Squeezed-film damping, Modal analysis, Macromodel

## INTRODUCTION

It is well-known that squeeze-film damping can affect the dynamics of microstructures. As shown in previous work on CISQFD with rigid structures [1-7], there is both a viscous component and a spring component of pressure forces. By using the CISQFD macromodels, which were either derived analytically [1,2] or calculated numerically [3], the dynamical models of MEMS structures can be accurately formulated and calculated. However, these studies are only applicable to *rigid* microstructures.

In this paper, we present an efficient and accurate method for modeling CISQFD for *flexible MEMS structures*, such as fixed-fixed beams, cantilevers and membranes, undergoing small amplitude oscillation. The approach is to combine structural modal analysis with numerical solution of the equation governing CISQFD, the *linearized Reynold's equation* [1]. In this work, we apply the same methodology as in [3], but with sinusoidally moving boundaries using shapes governed by the dynamical resonant mode shapes of a *flexible mechanical structure* (see Fig. 1 (a)). The method incorporates the effective modal spring constants and masses obtained from the modal analysis using Abaqus, as in [8]. From the distributed fluidic reaction forces on the applied moving boundaries in sinusoidal steady state, it is possible to extract an effective spring constant and damping coefficient due to CISQFD for any oscillation mode. We can then construct a concise second-order dynamical equation for a deformation mode of a flexible MEMS device incorporating both the CISQFD force parameters and the modal

spring constant and mass. The dynamics simulation results have been compared with experimental results for microbridge structures with different length-width ratios.

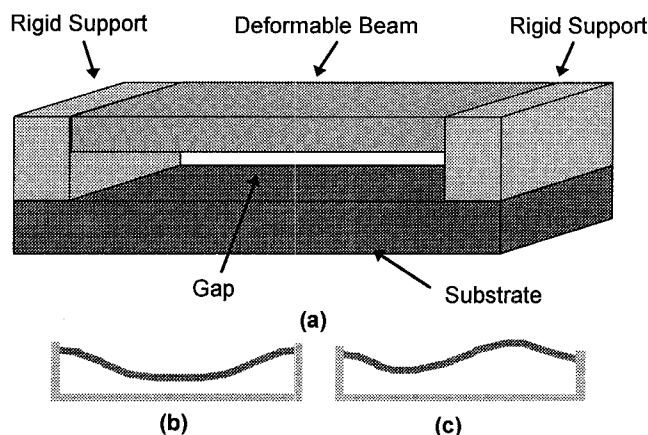


**Figure 1** (a) Schematic view of a flexible mechanical microstructure (a fixed-fixed beam). (b) and (c) are the first two dynamical resonant mode shapes of (a) obtained by modal analysis [8].

## THEORY DERIVATION

In previous work for a rigid plate moving normal to the substrate, the analytical form of the CISQFD spring constants and damping coefficients ( $k_a$  and  $c_a$  in Fig. 2) for circular and rectangular plates have been obtained by solving the linearized Reynold's equation [1,2], whose nondimensional form is

$$\nabla^2 \Theta - \sigma \frac{\partial \Theta}{\partial \tau} = \sigma \frac{\partial e}{\partial \tau} \quad (1)$$

$$\tau = \omega t ; e = \frac{\delta}{h_0} \cos \omega t ; \Theta = \frac{\Delta p}{P_a} ; \sigma = \frac{12 \mu L^2 \omega}{P_a h_0^2}$$

where  $\omega$  is the oscillation frequency,  $\tau$  is non-dimensional time,  $\delta$  is the amplitude of oscillation,  $\Delta p$  is the incremental pressure variation,  $\Theta$  is the normalized incremental pressure variation,  $L$  is the characteristic plate length,  $h_0$  is the gap thickness,  $\mu$  is viscosity,  $P_a$  is the ambient pressure and  $\sigma$  is the squeeze number.

Note that the forcing function,  $e$ , for this rigid-plate formulation is a function only of time, and the incremental pressure  $\Theta$  is zero on the perimeter of the plate. The s-plane transfer function  $T(s)$  for this rigid plate motion with the CISQFD effect can be formulated by adding the CISQFD spring

## 4A2.01

constant and damping coefficient into the structural parameters ( $m$  and  $k$  in Fig. 1), as shown below :

$$T(s) = \frac{Z(s)}{F_E(s)} = \frac{1}{s^2 m + s c_a + (k + k_a)} \quad (2)$$

where  $Z$  is the displacement of the moving plate normal to the substrate, and  $F_E$  is the external excitation force.

This transfer function gives an efficient and accurate way to examine the frequency response with CISQFD for rigid plate structures as presented in the previous studies [3-7]. Fig. 3 shows the typical responses of Eqn 2. Curve 1 is the response without CISQFD. Curve 2, which drops very fast, is the response with the air damping in ambient. Curve 3 is the response with CISQFD in low pressure or when the moving plate is perforated. Note the appearance of the resonance, shifted to higher frequency by the stiffness of the added air spring.

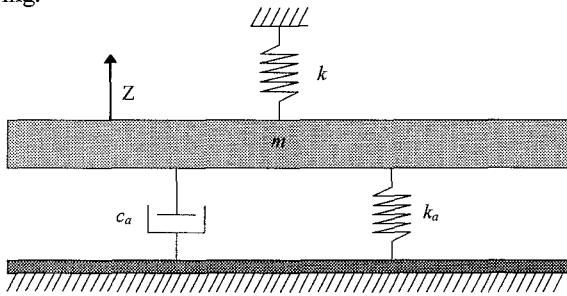


**Figure 2** Spring-mass-damper model with squeezed-film damping for rigid plates. For flexible structures represented with a modal coordinate, the  $k$ ,  $k_a$ ,  $c_a$  and  $Z$  are replaced with  $k_G$ ,  $k_{aG}$ ,  $c_{aG}$  and  $Q$ , respectively. (see Eqn. 2 and 9)

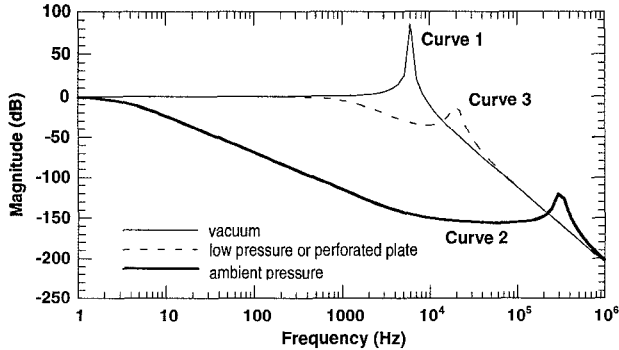


**Figure 3** Simulated dynamical responses of the rigid plate of Fig. 2 with and without air film damping effects [3].

For flexible MEMS structures, however, the moving-boundary forcing function imposed on the Reynold's equation is not only a function of time, but also has spatial dependence. Furthermore, the shape of a oscillating flexible structure is usually dominated by one mode, depending on the configuration of external excitation forces [8]. Therefore, it is feasible to solve the linearized Reynold's equation numerically with a moving boundary determined by the dominant oscillating mode shape. The modal parameters, such as oscillating mode shapes (eigenvectors), generalized spring constants, and generalized masses for each oscillation mode, can be obtained by

commercial structural dynamics finite-element codes (in this study, we use Abaqus). The equation of motion can be constructed by using the modal parameters :

$$M_G \{\ddot{q}\} + K_G \{q\} = -V^t \{F_P(V\{q\}, V\{\dot{q}\})\} + V^t \{F_E\} \quad (3)$$

where  $V$  is the  $N \times N$  modal matrix ( $N$  is the number of nodes after discretizing the moving flexible plate) which contain the eigenvectors (mode shapes) for each oscillation mode,  $M_G$  and  $K_G$  are the generalized mass and spring matrices ( $N \times N$ ) and are diagonal,  $F_P$  is the pressure force distribution ( $N \times 1$ ) along the flexible moving plate and is a function of both the displacement and velocity on each node of the plate,  $F_E$  is a vector ( $N \times 1$ ) representing the external excitation force, and  $\{q\}$  is a vector containing modal amplitude of each mode.

Since the dominant oscillation mode is of interest, Eqn. 3, which is a system of  $N$  2<sup>nd</sup> order differential equations, can be truncated into one 2<sup>nd</sup> order differential equation of the dominant oscillation mode, which, in the  $s$ -plane, becomes:

$$s^2 m_G Q(s) + k_G Q(s) = -\{v\}^t \{F_P(\{v\}Q(s), \{v\}sQ(s))\} + F_{EG}(s) \quad (4)$$

where  $Q(s)$  is the modal variable of the dominant mode,  $\{v\}$  is the corresponding eigenvector,  $k_G$  and  $m_G$ , are the corresponding generalized spring constant and generalized mass respectively, and  $F_{EG}$  is the generalized external force which excites the structure in the dominant mode.

Due to the assumption of small amplitude oscillation, the spring component ( $F_{Pc}$ ) and damping component ( $F_{Pd}$ ) of the CISQFD pressure reactant force on each node of the moving plate can be decoupled [2,3]. The equation of motion becomes :

$$s^2 m_G Q(s) + k_G Q(s) = -\{v\}^t \{F_{Pc}(\{v\}Q(s))\} - \{v\}^t \{F_{Pd}(\{v\}sQ(s))\} + F_{EG}(s) \quad (5)$$

In order to obtain the effective CISQFD spring constant and the damping coefficient numerically, we use the dominant oscillation mode shape as the sinusoidally moving boundary for the linearized Reynold's equation with a specific squeeze number (Eqn. 1), then integrate it in time until reaching steady state. The spring and damping forces on each node can be determined from the total node reaction force using the phase shift between the steady state local pressure force and the velocity on that node, as shown in Fig. 4. The effective CISQFD spring constant and damping coefficient on each node can be obtained from the decoupled node forces by dimensional analysis, as described in [3,4]. With the effective CISQFD parameters and eigenvector elements written explicitly, Eqn. 5 can be rewritten as:

$$s^2 m_G Q(s) + k_G Q(s) = -\{v_1 \dots v_N\} \begin{Bmatrix} k_{a1} v_1 \\ \vdots \\ k_{aN} v_N \end{Bmatrix} Q(s) - \{v_1 \dots v_N\} \begin{Bmatrix} c_{a1} v_1 \\ \vdots \\ c_{aN} v_N \end{Bmatrix} s Q(s) + F_{EG}(s) \quad (6)$$

where  $v_n$ 's are the elements of the eigenvector, and  $k_{an}$ 's and  $c_{an}$ 's are the effective spring constants and damping coefficients on each node.

These effective spring and damping parameters are then projected back onto the mode shape to determine an effective spring and damping force for the dominant mode. Thus the generalized CISQFD spring constant and damping coefficient for this oscillation mode are :

$$k_{aG} = \sum_n^N k_{an} v_n^2 ; \quad c_{aG} = \sum_n^N c_{an} v_n^2 \quad (7)$$

and Eqn. 6 can be simplified as

$$s^2 m_G Q(s) + k_G Q(s) = -k_{aG} Q(s) - s c_{aG} Q(s) + F_{EG}(s) \quad (8)$$

From Eqn. 8 we obtain the transfer function of this oscillation mode with the effective generalized CISQFD parameters, as shown in Eqn. 9.

$$T(s) = \frac{Q(s)}{F_{EG}(s)} = \frac{1}{s^2 m_G + s c_{aG} + (k_G + k_{aG})} \quad (9)$$

Note that Eqn. 9 has the same form as Eqn. 2, and the mass-spring-damper model shown in Fig. 2 is equivalent to this new transfer function of the dominant oscillation mode. The main difference between Eqn. 2 and Eqn. 9 is that the latter represents the dynamics in the modal coordinate  $Q(s)$  which is the variable describing the motion with dominant mode shape. Similar to the rigid-plate case, the frequency response with CISQFD for this dominant oscillation mode can be calculated by Eqn. 9.

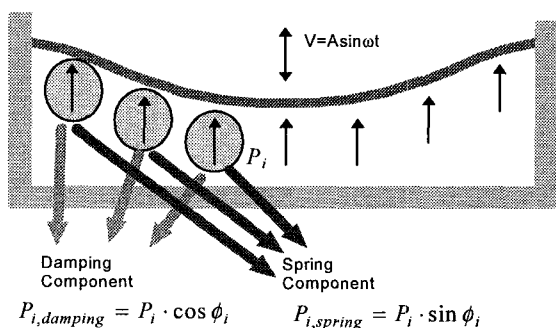


**Figure 4** Schematic view of a flexible MEMS structure (a fixed-fixed beam) with squeezed-film damping. The reaction pressure force due to CISQFD on each node can be decoupled into spring and damping components.  $P_i$  is the total local reaction pressure on the  $i^{\text{th}}$  node and  $\phi_i$  is the phase difference between the sinusoidal input velocity and  $P_i$  on the  $i^{\text{th}}$  node.

We calculated the generalized CISQFD parameters repeatedly for a wide range of different squeeze numbers, then obtained the squeeze number dependence of the pressure force components. Fig. 5 shows the spring and damping components vs. squeeze number on different nodes of a microbridge with aspect ratio 10 (length/width) operating in its fundamental oscillation mode. In

this calculation, the mesh for solving the linearized Reynold's equation is based on the two-dimensional structural mesh of the fixed-fixed beam from Abaqus. We used a symmetric finite difference formulation (zero-flux boundary) for the incremental pressure on the nodes located on the fixed ends of the beam, and the incremental pressure on the other two edges of the beam is zero. Fig. 6 shows the squeeze number dependence of the resulting generalized spring and damping forces for fixed-fixed beam structures with aspect ratio 10. Since Fig. 6 is non-dimensional, this generic plot is valid for any thin fixed-fixed beam with aspect ratio 10. Thus it is possible to create a macromodel database of CISQFD by doing a series of generic calculations for different aspect ratios. This generic calculation is also applicable to other typical MEMS flexible structures, such as cantilevers and membranes.

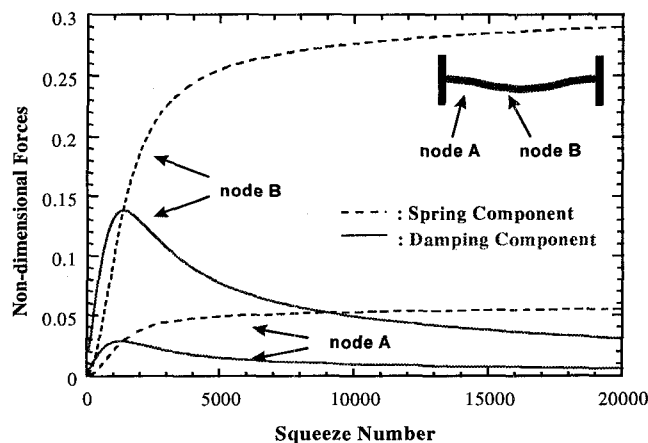


**Figure 5** Nondimensional spring and damping forces on selected nodes of a fixed-fixed beam (aspect ratio 10) in the fundamental oscillation mode. Note that the pressure force components on node A are smaller than those on node B because the relative displacement of node A is smaller than node B.

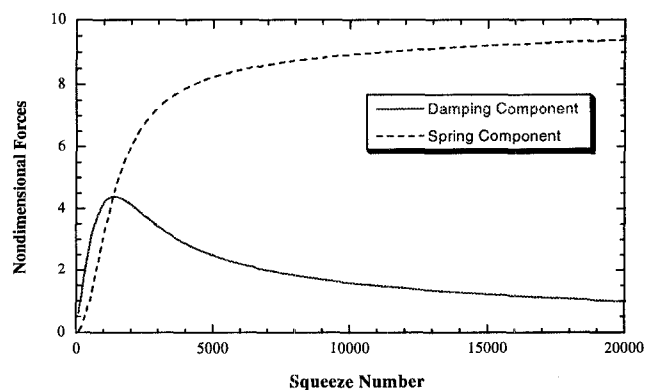


**Figure 6** Nondimensional generalized spring and damping forces of the fundamental oscillation mode for a fixed-fixed beam with aspect ratio 10.

## SIMULATION AND EXPERIMENT RESULTS

Simulation results of resonance shift and quality factor are consistent with experimental results, as described below. The data of Figs 7 and 8 are from the fundamental mode of two

#### 4A2.01

polysilicon/nitride composite microrelay beams, described separately in [9], to which a static 7-volt bias has been applied in addition to a small ac excitation so as to drive the resonance. Because of the static bias, it was necessary to include the well-known spring-softening effect, and this was done in our simulation. A slip-flow correction to the viscosity was also employed [7]. The quality factor  $Q$  (in both figures) is relatively independent of the beam's constitutive properties, but is a strong function of ambient pressure due to the damping force component on the fundamental mode. Agreement with experiment is excellent down to 1 mbar, at which point the intrinsic losses in the beam resonance limit the  $Q$ , while the CISQFD calculation predicts a continuing increase in  $Q$ . The resonant frequency (in both figures) depends directly on the beam's constitutive properties. Here, the agreement between the calculated and measured resonant frequency was to within about 5%. In order to demonstrate the perturbation of the resonance by the air damping spring force, the modal stiffness in the simulation was arbitrarily reduced slightly so that the low-pressure resonant frequency agreed with the experiment value. The shift to higher frequencies produced by the CISQFD spring force was calculated from pressures up to 20 mbar.

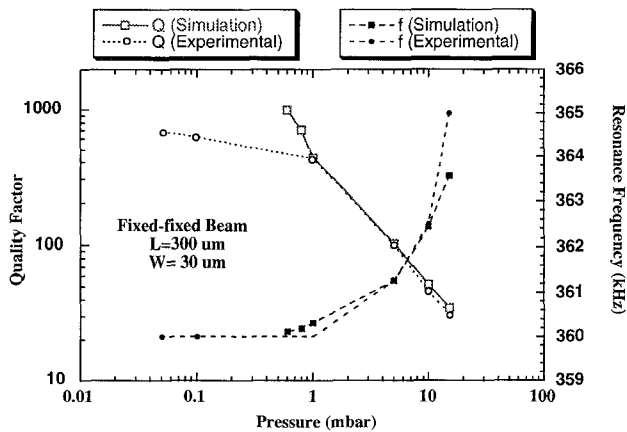


Figure 7 Quality factor and resonance shift vs. pressure for a 300  $\mu\text{m}$  long microrelay beam in its fundamental oscillation mode.

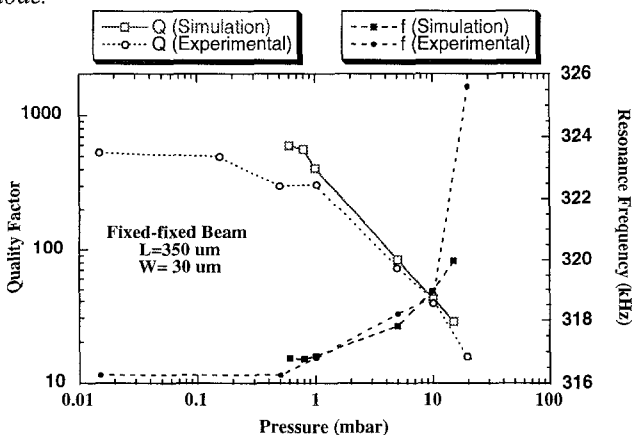


Figure 8 Quality factor and resonance shift vs. pressure for a 350  $\mu\text{m}$  long microrelay beam in its fundamental oscillation mode.

#### SUMMARY

A new technique to calculate the small amplitude CISQFD spring constant and damping coefficient for flexible MEMS structures has been demonstrated. The theory, which is based on a structural modal analysis and CISQFD transient simulation, have been explained and derived. For a specific oscillation mode, the effective CISQFD parameters (macromodel) of flexible MEMS structures are obtained by this technique and thus the dynamics response with CISQFD can be analyzed efficiently and accurately. Simulation and experimental results of a fixed-fixed-beam microrelay structure shows excellent agreement for both quality factor and resonant frequency. Non-dimensional numerical results for the CISQFD parameter also provide generic CISQFD macromodels for different typical flexible MEMS structures.

#### ACKNOWLEDGMENT

This work was funded in part by the Semiconductor Research Corporation. The authors wish to thank Dr. G. K. Ananthasuresh for useful discussion of modal analysis.

#### REFERENCE

- [1] W. E. Langlois, "Isothermal Squeeze Films," *Quar. Applied Mathematics*, Vol. XX, No. 2, 1962, pp. 131-150.
- [2] J. J. Blech, "On Isothermal Squeeze Films," *Journal of Lubrication Technology*, Vol. 105, 1983, pp. 615-620.
- [3] Y.-J. Yang and S. D. Senturia, "Numerical Simulation of Compressible Squeezed-Film Damping," *Tech. Digest, Solid State Sensor and Actuator Workshop Hilton Head Island, SC, June 1996*, pp. 76-79.
- [4] M. Andrews, I. Harris and G. Turner, "A Comparison of Squeeze-film Theory with Measurements on A Microstructure," *Sensors and Actuators A*, Vol. A36, 1993, pp. 79-87.
- [5] J. B. Starr, "Squeeze-film Damping in Solid-State Accelerometers," *Tech. Digest, IEEE Solid State Sensor and Actuator Workshop, Hilton Head Island, SC, June 1990*, pp. 44-47.
- [6] M. Andrews, G. Turner, P. Harris and I. Harris, "A Resonant Pressure Sensor Based on A Squeezed Film of Gas," *Sensors and Actuators A*, Vol. A36, 1993, pp. 219-226.
- [7] T. Veijola, H. Kuisma, J. Lahdenperä and T. Ryhänen, "Equivalent-circuit model of the squeezed gas film in a silicon accelerometer," *Sensors and Actuators A*, Vol. A48, 1995, pp. 239-248.
- [8] G. K. Ananthasuresh, R. K. Gupta and S. D. Senturia, "An Approach to Macromodeling of MEMS for Nonlinear Dynamic Simulation," *ASME International Mechanical Engineering Congress and Exposition, Symposium on MEMS, Atlanta, GA, Nov. 1996*, pp. 18-22.
- [9] M.-A. Gretillat, P. Thiebaud, N. F. de Rooij and C. Linder, "Electrostatic Polysilicon Microrelays Integrated with MOSFETs," *Proc. IEEE MEMS Workshop 94, Oiso, Japan (1994)*, pp. 97-101.